

휴대폰 안테나와 사용자 머리와의 전자기 상호작용: 해부학적 머리와 다층구형 머리 결과비교

김 강 욱
경북대학교 전자전기컴퓨터학부

Electromagnetic Interactions between Handset Antennas and Human Head: Anatomical Head vs. Multi-layered Spherical Head

Kang W. Kim
School of Electrical Engineering and Computer Science, Kyungpook National University

ABSTRACT

An anatomical head and a multi-layered spherical head with a half-wave handset antenna have been analyzed and compared using the Finite-Difference Time-Domain (FDTD) and the Eigenfunction Expansion Method (EEM), respectively. The analysis shows that results from a simple spherical head with a half-wave antenna can be used to predict the main antenna radiation patterns as well as estimates of the peak SAR in a handset user's head. Various representative design data are presented using a six-layered spherical head with a half-wave antenna at 900 MHz.

1. Introduction

Comprehensive understanding of EM interactions between human and handheld antennas is essential for handheld antenna design and for prevention of health hazard. Since the human head is usually located in the near-field region of the antenna, the performance of the antenna may be severely affected. Also, significant portion of the antenna-delivered power may be absorbed in the head. Antenna-head interaction studies have been extensively performed using various numerical techniques such as the Finite-Difference Time-Domain (FDTD) method [1,2,3], the Method of Moments (MoM) [4], and the Eigenfunction Expansion Method (EEM) [5,6]. The FDTD method, which is the most popular numerical technique, uses the anatomical human tissue model based on the Magnetic Resonance Image (MRI) [2,3]. Recently, the EEM has been developed to perform a systematic evaluation of the EM interactions between antennas and a multi-layered spherical head [5,6]. These numerical techniques provide important

antenna design parameters such as the antenna radiation patterns, antenna impedance, and specific absorption rate (SAR) in the presence of the human head.

In this paper, the near- and far-field patterns of a half-wave antenna with the anatomical head using FDTD are compared with those of the spherical head using EEM. The results obtained with the spherical head can be used to provide useful estimates for various antenna design purposes. Finally, various representative results obtained with a six-layered spherical head are presented. In this paper, computation results at 900 MHz are presented.

2. Computation Methodology

EEM: The eigenfunction expansion method (EEM), which uses the dyadic Green's function, is based on the exact scattering solution of infinitesimal dipoles. The scattered field is expressed as a series expansion of the spherical vector wave functions. A half-wave antenna is simulated by a series of infinitesimal

electric dipoles with an appropriate current distribution. To accurately account for EM interactions between antennas and the multi-layered sphere, the hybridization of EEM and the method of moments (MoM) has been performed. Using this hybridization, the current distribution on the antenna in the presence of a spherical head has been determined efficiently; the only unknowns are antenna surface current elements since the scattered dyadic Green's function is provided by EEM.

FDTD Algorithm: The FDTD algorithm is derived from Maxwell's time-domain integral equations. By placing the field components on the "Yee" unit cell, the equations are discretized to provide second-order accuracy [7]. In the FDTD calculation, all field values are initially set to zero. A source is introduced by setting a voltage at the antenna feed point and computing from it the source electric field. The electric and magnetic field values are then calculated using a leap-frog scheme; i.e. the magnetic field is first calculated at a time $t = n+1/2$, and the electric field is subsequently calculated at $t = n+1$. Continuity of fields is naturally enforced at a dielectric boundary in this algorithm. However, at the conductor interface, the tangential E field must be explicitly set to zero. At the outer boundary of the computation, perfectly matched layer (PML) boundary conditions [8] are typically applied.

3. Results with Anatomical and Multi-layered Spherical Heads

Near- and far-field patterns of the half-wave antenna at 900 MHz in the presence of an anatomical head are compared with those of the spherical head. The anatomical head and the multi-layered spherical head have been analyzed by FDTD and EEM, respectively. The anatomical head is composed of seven biological tissues—skin, bone, brain, muscle, humor, lens, cornea—as shown in Figs. 1(a) and (b). The

permittivity and the conductivity of the tissues at 900 MHz are taken from [2]. These parameters can also be obtained using the multiple Cole-Cole dispersion equation and the corresponding parameters in [9]. The half-wave antenna is located at 2 cm away from the outer edge of the head. The grid cell size for the FDTD calculation is $0.02 \lambda_0$ (~ 6.7 mm). In order to compare with this anatomical head, a three-layered spherical head composed of skin, bone, and brain is used to form the dominant biological tissues in a handset user's head. The thickness of the skin and bone layer is about 6.7 mm, similar to the anatomical head model. The diameter of the sphere is 17.3 cm. Also, a homogeneous head with the electrical parameters of brain is also analyzed.

The gain patterns of the half-wave antenna in the presence of the anatomical, homogeneous, and three-layered spherical heads are compared in Figs. 2 (a) and (b). The forward gain patterns from all three configurations agree very well, but the backward gain with the anatomical head is ~ 3 dB lower than that with the three-layered head. This lower gain with the anatomical head might be attributed to the non-spherical head shape. However, the spherical head model predicts the correct null locations, and also provide very similar radiation patterns.

Next, the total electric field distributions inside the three head configurations are compared in Fig. 2(c). The distance is measured from the outer edge of the head. The field distributions of the three-layered and homogeneous heads are similar. The field strength in the anatomical head is slightly lower than the others, but overall tendency looks similar. Important observation is that electric field strength near surface of the head agrees very well for all three heads. This might suggest that the spherical head model can be used for a reasonable estimate of the peak electric field or the peak SAR in the head. SAR in the head can be obtained by multiplying the tissue

conductivity to the square of the electric field divided by the mass density of the tissue (i.e., $SAR = \sigma|E|^2/2\rho$). Since the total electric field approximately decays exponentially inside the head, peak SAR will occur where the conductivity of the tissue is higher. Since the electric field distributions near the head surface for three head configurations are similar, reasonably accurate estimation of peak SAR may be obtained using even a simple homogeneous spherical head model for a variety of antenna designs. A multi-layered spherical head model, however, serves a better approximation of the anatomical head, especially for investigation of effects relating to the thin biological layers [5,6].

4. Representative Design Data

Finally, representative design data are provided using a six-layered spherical head (diameter 18 cm) with a half-wave dipole antenna. The simulated tissues are skin (1 mm), fat (1.4 mm), bone (4.1 mm), dura (0.5 mm), cerebrospinal fluid (CSF; 2 mm), and brain. A half-wave antenna is located at 2 cm away from the spherical head. Gain patterns without and with the head in the horizontal plane (y - z plane) are shown in Fig. 3(a). In the figure, the gain patterns are obtained as varying the distance (x_1) between the center of the dipole antenna and the head center. One can observe that, in the presence of the head, the antenna gain can be lowered as much as ~ 5.7 dB (with $x_1=0$) as compared with the free-space dipole antenna gain. This reduction of gain is seen along $\theta=120^\circ$ in Fig. 3(a). As x_1 is higher, the antenna gain recovers that of free-space. The specific absorption rate (SAR) distribution in the head along the z -axis with 1 W of the antenna delivered power (with $x_1=0$) is shown in Fig. 3(b). In the figure, the solid line represents the unaveraged SAR while the dashed line represents the 1-g averaged SAR. The unaveraged maximum SAR occurs at the CSF layer, and the second peak SAR at

the skin layer. Also, note that the 1-g averaged peak SAR is much smaller than that of the unaveraged SAR. The absorbed powers in the head are 43.9% with $x_1=0$ cm, 30.1% with $x_1=5$ cm, and 14.8% with $x_1=10$ cm. The total absorbed power in the head with $x_1=0$ is plotted as a function of the antenna-head separation distance and the radius of the spherical head in Fig. 3(c).

References

- [1] M. A. Jensen and Y. Rahmat-Samii, "EM Interaction of Handset Antennas and a Human in Personal Communications," *Proc. IEEE*, Vol. 83, No. 1, pp. 7-17, Jan. 1995
- [2] V. Hombach, K. Meier, M. Burkhardt, E. Kuhn, N. Kuster, "The Dependence of EM Energy Absorption Upon Human Head Modeling at 900 MHz," *IEEE Trans. Microwave Theory Tech.*, Vol. 44, pp. 1865-1873, Oct. 1996
- [3] O. P. Gandhi, G. Lazzi, C.M. Furse, "Electromagnetic Absorption in the Human Head and Neck for Mobile Telephones at 835 and 1900 MHz," *IEEE Trans. Microwave Theory Tech.*, Vol. 44, pp. 1884-1897, Oct. 1996
- [4] J. S. Colburn and Y. Rahmat-Samii, "Electromagnetic Scattering and Radiation Involving Dielectric Objects," *J. Electromagnetic Waves and Applications*, Vol. 9, No. 10, pp. 1249-77, 1995
- [5] K. W. Kim and Y. Rahmat-Samii, "Antennas and Humans in Personal Communications: An Engineering Approach to the Interaction Evaluation," *Proceedings of the IEEE Engineering in Medicine and Biology Society*, Chicago, pp. 2488-2491, October, 1997
- [6] Y. Rahmat-Samii, K. W. Kim, M. Jensen, K. Fujimoto, and O. Edvardsson, "Antennas and Humans in Personal Communications: Application of Modern EM Computational Techniques (Chapter 7.1)," *Book Chapter in Mobile Antenna Systems Handbook*, 2nd Edition, 2001 Artech House, Inc., Edited by K. Fujimoto and J. R. James
- [7] A. Taflove, *Computational Electromagnetics: The Finite-Difference Time-Domain Method*, Boston: Artech House, Inc., 1995
- [8] J. -P. Berenger, "A perfectly matched layer for the absorption of electromagnetic waves," *J. Computational Physics*, vol. 114, pp. 185-200, 1994
- [9] S. Gabriel, R. W. Lau, and C. Gabriel, "The Dielectric Properties of Biological Tissues: III. Parametric Models for the Dielectric Spectrum of Tissues," *Phys. Med. Biol.* 41, 2271-2293, November 1996

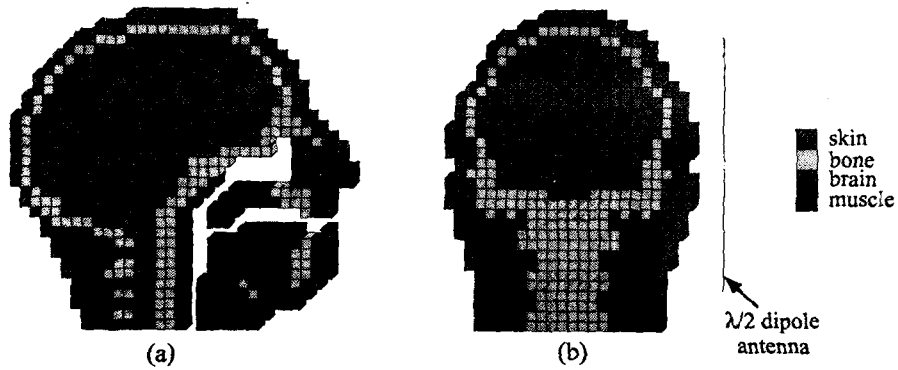


Figure 1 Cross sectional view of the anatomical head for the FDTD computation:
(a) a sagittal cut; (b) a front cut.

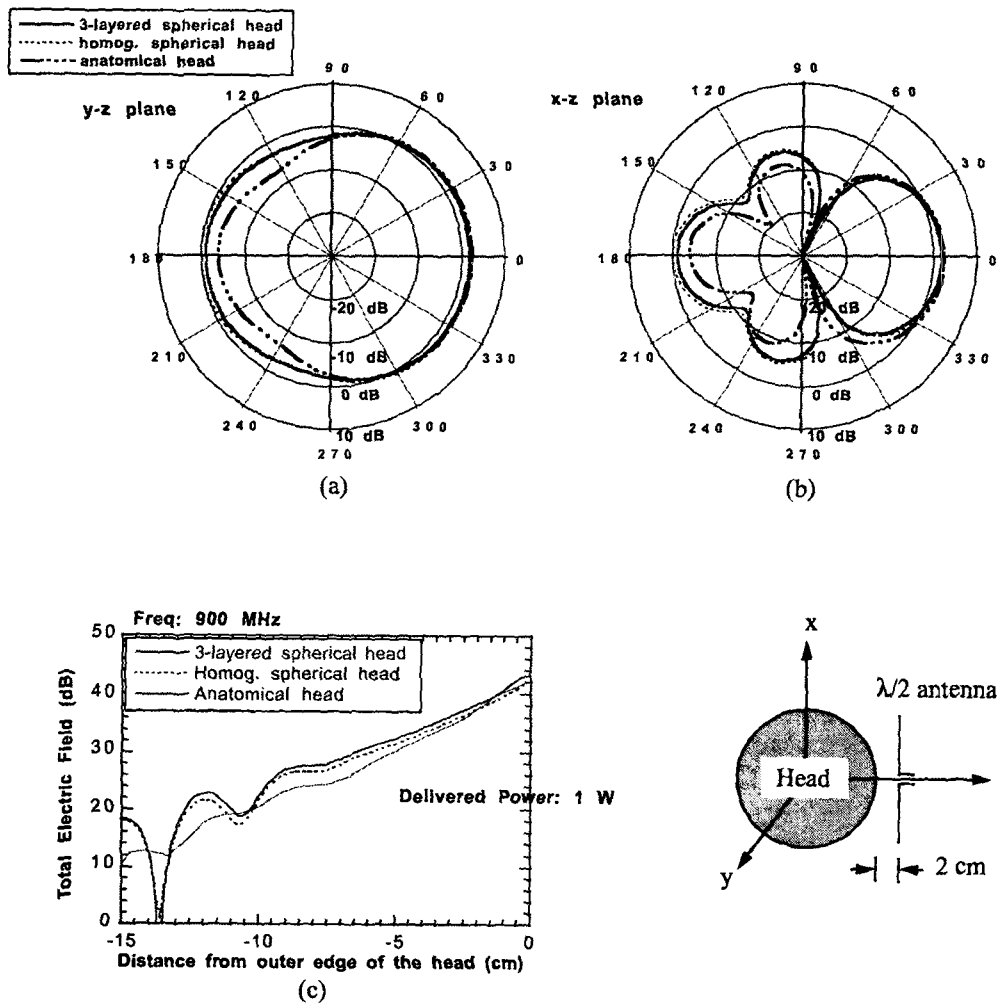


Figure 2 Comparison of near- and far-field patterns of the spherical head and anatomical head: (a) gain pattern in the y-z plane; (b) gain pattern in the x-z plane; (c) total electric field inside the head along the z-axis ($20 \log|E|$). The antenna delivered power is set at 1 W.

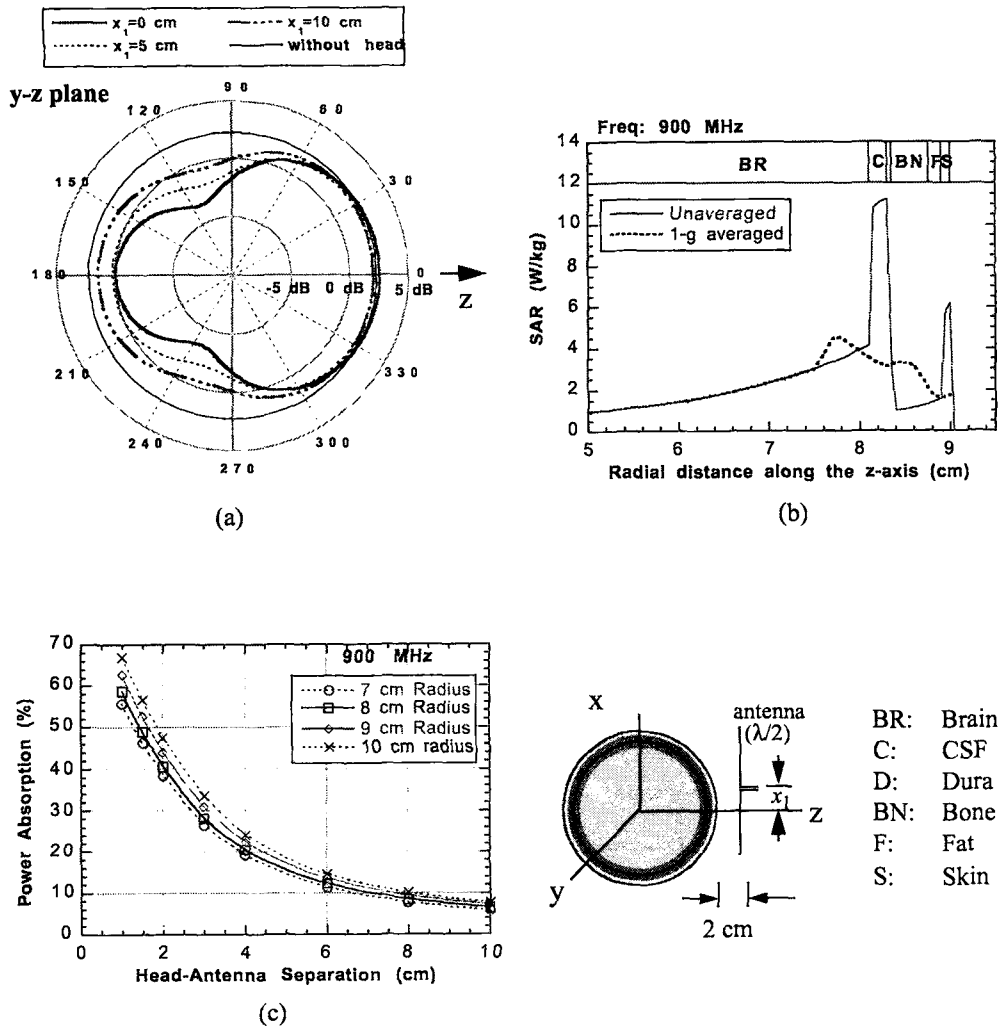


Figure 3 (a) Gain patterns of a $\lambda/2$ antenna with and without a six-layered spherical head as changing the antenna vertical location (x_1) in y-z plane; (b) SAR distribution with $x_1=0$ —1-g averaged and unaveraged—along the z axis; (c) total power absorption in the spherical head as function of the head-antenna separation distance and head radius. Operating frequency of antenna is 900 MHz.